

# HYBRID CONTROLLED BASE-ISOLATION SYSTEM WITH SEMI-ACTIVE MAGNETORHEOLOGICAL DAMPER AND ROLLING PENDULUM SYSTEM

P. Y. Lin<sup>1</sup>, P. N. Roschke<sup>2</sup>, C. H. Loh<sup>1</sup> and C. P. Cheng<sup>1</sup>

<sup>1</sup>*National Center for Research on Earthquake Engineering, Taipei, Taiwan*

<sup>2</sup>*Department of Civil Engineering, Texas A&M University, College Station, Texas*

[pylin@ncree.gov.tw](mailto:pylin@ncree.gov.tw), [roschke@civilmail.tamu.edu](mailto:roschke@civilmail.tamu.edu), [loh@ncree.gov.tw](mailto:loh@ncree.gov.tw), [benjamin@ncree.gov.tw](mailto:benjamin@ncree.gov.tw)

## Abstract

A series of large-scale experimental tests is conducted on a mass equipped with a hybrid controlled base-isolation system that consists of rolling pendulum system (RPS) and a 20 kN magnetorheological (MR) damper. The 12-ton mass and its hybrid isolation system are subjected to various intensities of near- and far-fault earthquakes on a large shake table. Fuzzy controllers use feedback from displacement, and acceleration transducers attached to the structure to modulate resistance of the semi-active damper to motion. Results from various types of passive and semi-active control strategies are summarized and compared. The study shows that a combination of rolling pendulum system and an adjustable MR damper can provide robust control of vibration for large civil engineering structures that need protection from a wide range of seismic events. Low power consumption, direct feedback, high reliability, energy dissipation, and fail-safe operation are validated in this study.

## INTRODUCTION

While standard base isolation techniques such as insertion of rubber bearings between the ground and a structure that is to be protected have been applied for a number of years [*Naeim F*], the addition of supplemental damping devices is being considered for large structures in order to create more robust resistance to a variety of earthquake characteristics. One recent comprehensive study [*Chang SP*] used experimental and analytical methods to determine effectiveness of using lead-rubber or sliding bearings along with friction and viscous dampers for isolation of rigid structures. Supplemental passive damping devices have been found to be effective in reducing both displacement and base shear for structures that have moderately long periods.

Other researchers are studying the ability of semi-active devices to reduce vibrations in structures. Very small power consumption, high reliability and a fail-safe mechanism make semi-active control one of the more promising approaches for the mitigation of damage due to seismic events in civil engineering structures. There are fundamentally two types of semi-active control devices. The first type uses a mechanical system to alter behavior of the control device; examples of such systems

include the variable damping device [*Sadek, F*][*Symans MD*], semi-active hydraulic damper [*Kurata N*][*Niwa N,*] and a variable stiffness system [*Kobori T*]. The basic approach is to use a variable valve to modify damping and stiffness of the damper. The second type of semi-active control device uses a controllable fluid, such as electrorheological (ER) [*Burton SA*] or magnetorheological (MR) fluid [*Spencer, Jr BF*] [*Lin PY*]. In this case an applied field that is electric or magnetic changes mechanical properties of the fluid and controls force in the damper.

The latter technique, which involves MR damper technology, is receiving a great deal of attention among researchers investigating control of large civil engineering structures. An MR damper resembles an ordinary linear viscous damper except that the cylinder of the damper is filled with a special fluid that contains very small polarizable particles. Viscosity of the fluid can be changed very quickly from a liquid to a semi-solid and vice versa. This is accomplished by adjusting the magnitude of the magnetic field produced by a coil wrapped around the piston head of the damper. When no current is supplied to the coil, an MR damper behaves in a manner that is similar to that of an ordinary viscous damper. On the other hand, when current is sent through the coil, fluid inside the damper becomes semi-solid and its yield strength depends on the applied current [*Chang CC*]. Since the control force is not applied directly to the structure by the damper, but rather only the resistance of the damper is adjusted, control instability does not occur and only a small amount of energy is required. Therefore, an MR damper is a reliable and fail-safe device.

This study makes use of a supplemental MR damper in a large structure that is equipped with the rolling pendulum system as the base-isolation system in a laboratory. The goal is to exploit the reliability and simplicity of a traditional base isolator with another reliable device that is able to change its characteristics within milliseconds. Rapid adjustment of a large MR damper to its surroundings allows the hybrid base-isolation system to provide safe and effective filtering of a broad range of motions from near- and far-fault seismic events.

In what follows a testing program is carried out with a set of fuzzy logic controllers that use direct feedback of readily available data concerning motion of a single degree of freedom structure. The experimental structure as well as data acquisition and control hardware are described in Section 2. Development of three semi-active fuzzy controllers for the hybrid base isolation system is discussed next. The final sections present and analyze results from extensive experiments on a large shake table.

## **EXPERIMENTAL MODEL**

In this study, a base-isolated structure with rolling pendulum system and a 20 kN MR damper is tested on a shake table. Unlike the traditional isolators, such as high damping rubber bearing (HDRB) [*Lin PY*] or friction pendulum bearing[ *Wang, Y. P.*], the rolling pendulum system (RPS) is used in this study. In this study, the adjustable MR damper is the main energy absorber of the hybrid base-isolation system. As results, the damping force or friction force of the isolator is the fewer the better. The fewer resistance of the isolator the more controllable range of the semi-active controlled base-isolation system, as the isolator is not adjustable. The goal is to verify effectiveness of the hybrid control system with physical hardware and real-time processing requirements. Figure 1 shows a schematic drawing of the experimental setup. The isolated structure is constructed with a steel frame and lead blocks that provide a mass of 12 ton. The natural period of the rolling pendulum system is selected as 2.77 sec. Ends of the 20 kN MR damper are securely attached to the top surface of the shake table

and the side of the isolated structure.

An array of LVDTs, accelerometers, load cells and a thermal couple are used to measure the displacement, absolute acceleration, force and temperature, respectively, at salient locations on the experimental structure. Figure 2 shows locations of the experimental sensors. Displacements and accelerations of the base-isolated system are grouped into three levels: base of the rolling pendulum system (D0, A0), base of the isolated structure (D1, A1) and top of the isolated structure (D2, A2). Two LVDTs are placed at each level in order to measure both transverse and accidental torsional response. An additional LVDT is used to measure displacement response of the piston relative to the cylinder of the MR damper (Dmr). One additional accelerometer provides information concerning the piston of the MR damper.

A load cell (Lmr) is attached in-line with the axis of the MR damper in order to measure axial force. Finally, since temperature of the MR fluid is an important factor for reliable operation of the damper, one thermal couple (Tmr) is attached to the surface of the by-pass cylinder of the MR damper. Time histories of recorded earthquakes are feed into a computer that controls the shake table. Due to interaction between the table and test structure, a trial and error process of several iterations of the earthquake motion is used to compensate for the interaction so that a close approximation to the desired base motion is obtained.

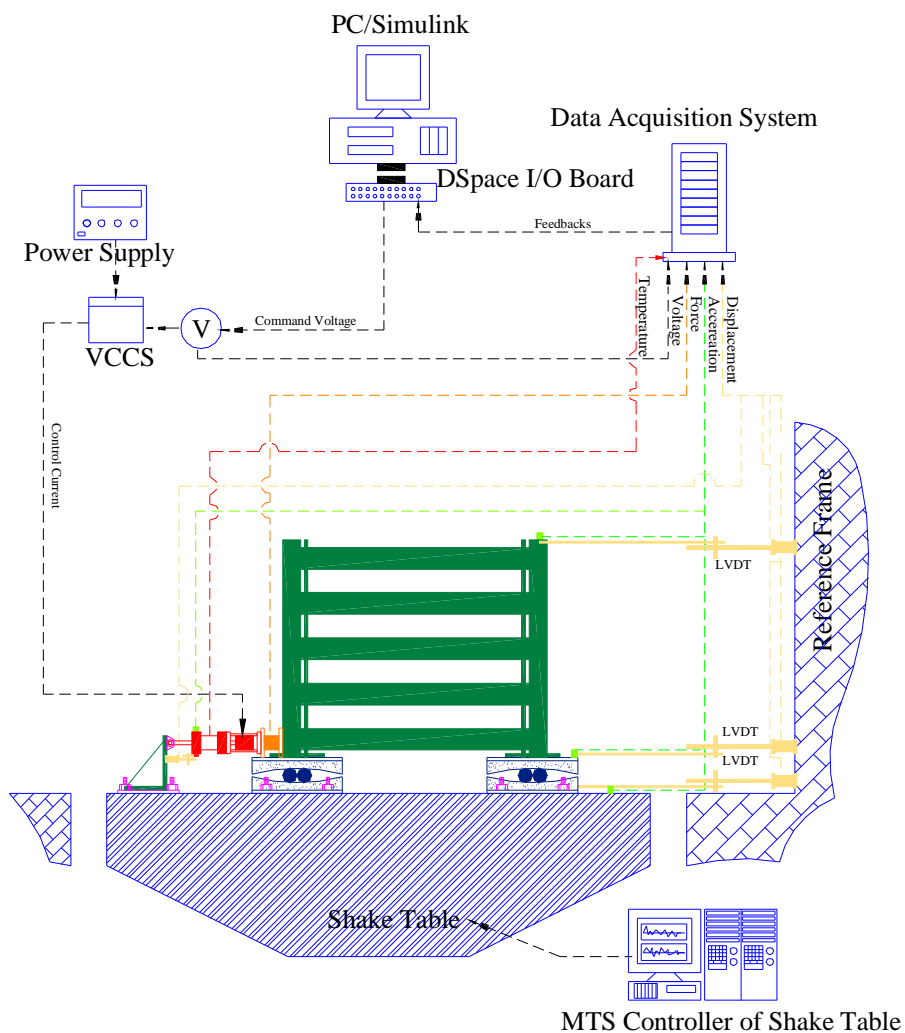


Figure 1: Experimental setup of test structure.

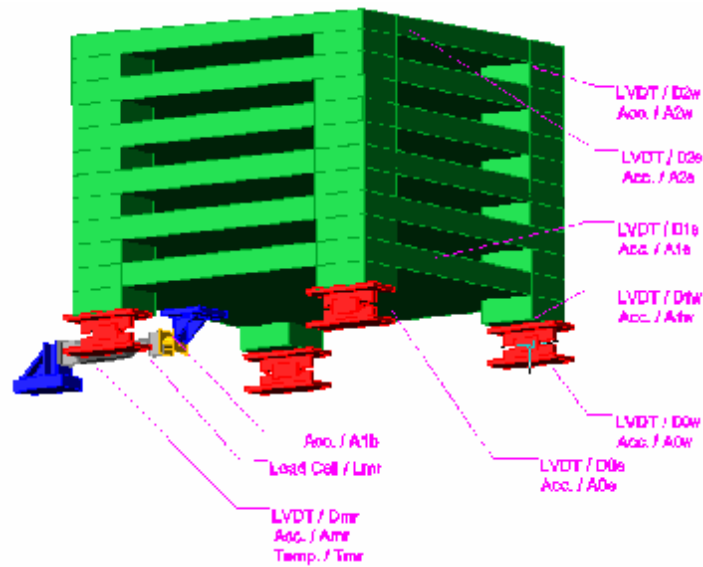


Figure 2: Configuration of experimental sensors

## DESIGN OF SEMI-ACTIVE CONTROLLERS

The semi-active control device used in this study is the 20 kN MR damper. Although its resistance to motion can be changed on command, it can not be treated like an active actuator for purposes of numerical simulation. Moreover, traditional active control algorithms cannot be directly applied to this hybrid control system. Therefore, semi-active controllers are developed in the context of the nonlinear base-isolated structure with rolling pendulum system and MR damper subcomponents. Fuzzy logic is used to map an input space to an output space by means of if-then rules [*Fuzzy Logic Toolbox Users Guide*]. Control components of the input signal are transformed into linguistic values through a fuzzification interface at each time step. Use of a fuzzy controller is advantageous in that performance is not overly sensitive to changes in the input signal. For output the mapped linguistic values are transformed into numerical values through a defuzzification interface.

Design of a fuzzy logic controller is separated into three parts: (1) use a fuzzy inference system (FIS) editor to define the number of input and output variables and choose the type of inference to be used; (2) define membership functions for the input and output variables; and (3) define if-then rules. In this study, a trial and error process results in the use of two inputs (displacement and acceleration) and one output (voltage) variable. Next, triangular membership functions and the range of their variables are defined for each input and output variable. Finally, the if-then rules are edited so as to connect each input and output

For semi-active controller, S3, the absolute acceleration and relative displacement are selected as inputs, and the output is the command voltage. The number of membership functions used for the inputs are five and six, while seven membership function are used for the output. The first input, absolute acceleration, uses "PH", "PS", "Z", "NS" and "NH" the second input, relative displacement, uses "PH", "PB", "PS", "NS", "NB" and "NH" the output variable, force, uses "PH", "PB", "PS", "Z",

“NS”, “NB” and “NH”. Figure 3 (a), (b) and (c) show the result of applying the input and output membership functions over the whole range of the input variables for semi-active control case “S3”.

The design approach for this case is to control both the absolute acceleration and the relative displacement. As result, it divides the response of the isolation system into three kinds. First, when the absolute acceleration is huge, the command voltage is small when relative displacement is small and big when the relative displacement is huge. In this situation, the command voltage is suppressed to prevent exciting the acceleration responses except when the relative displacement is also huge. Secondly, when the absolute acceleration is small, the command voltage is increase with the relative displacement, and as huge as possible. In short word, the command voltage is as huge as possible except the small response zone. Thirdly, when the absolute acceleration is almost zero, the command voltage is zero when relative displacement is small and small when the relative displacement is big and huge. This part provides a zero command voltage belt around tiny acceleration responses. It can force the MR damper to be soft when the excitation is over.

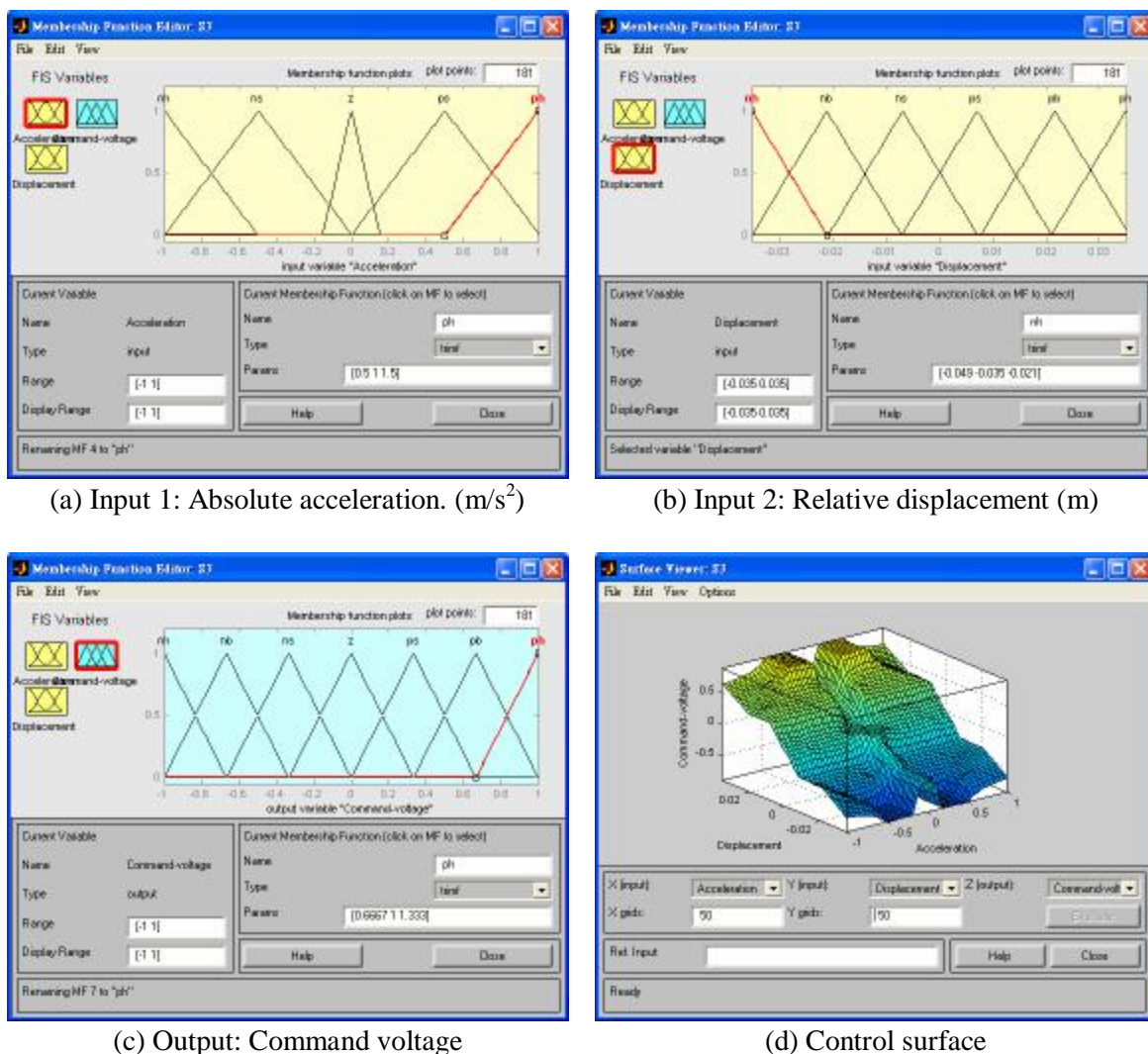


Figure 3: Input and output membership functions of semi-active control surface “S3”

Figure 3 (d) shows the control surface of semi-active control case “S3”. According to the figure, the

output has a zero plane when the inputs are small. This represents a command of zero volts when the structure is at rest. If the absolute acceleration is not large, i.e. less than one-half of the limit value, the output command is drastically changed with respect to a variation of the relative displacement. In this case it outputs a larger command to control the relative displacement, since control of absolute acceleration is not a problem. On the other hand, if the absolute acceleration is large, i.e. more than one-half of the limit value, the output command is “smoothly” changed with the relative displacement. This results in an output of smaller voltage to control the relative displacement, since application of a larger output voltage increases the absolute acceleration.

For this case ranges of the absolute acceleration and relative displacement are selected to be  $-1\sim 1$  m/s<sup>2</sup> and  $-0.035\sim 0.035$  m, respectively. When the magnitude of the input lies outside of its range, the boundary value is used. Also, during numerical simulation and for a real application, a saturation block is used to prevent undesirable overshooting.

### SHAKE TABLE TESTS

After preliminary numerical simulations are performed to show that fuzzy control of a hybrid base-isolation system that is equipped with rolling pendulum pads and an MR damper can be effective in reducing displacement and acceleration, an experimental testing program is conducted. Figure 4 shows the photo of the 12-ton test structure in NCREE, 2003. A range of earthquake time histories are used to quantify levels of control for passive and semi-active control options (see Table 1). Excitation records that are investigated include El Centro, Kobe and Chi-Chi (at stations TCU052 and TCU068). Fast Fourier transforms (FFTs) of the time histories show that frequency content of the El Centro earthquake is relatively wide (0~8 Hz) while the near-fault Kobe earthquake has significant low frequency components. Similarly, Chi-Chi earthquake accelerations are recorded very close to a fault, and the time history of ground acceleration includes a very low frequency wave. Peak ground acceleration (PGA) levels of 50, 100, 200, 300 and 400 gal are specified for the shake table. The maximum PGA that is applied by the shake table for each earthquake is limited by the 50 mm displacement capacity of the MR damper.



Figure 4: Photo of the 12-ton test structure --- Hybrid controlled base-isolation system composed with

the rolling pendulum system and MR damper.

Two passive and one semi-active cases are employed for each test on the shake table. All the cases employ four rolling pendulum pads along with the 20 kN MR damper. The passive cases, termed “P-off”, which uses zero voltage is used to simulate a failure situation in which the MR damper undergoes a loss of power. The passive cases, termed “P-on” which uses one voltage is used to simulate the full power situation of the MR damper. The final series of cases, labeled “Semi-active,” uses feedback from the transducers and the semi-active controllers (S3) to adjust resistance of the MR damper.

Table 1: Excitations used in shake table tests

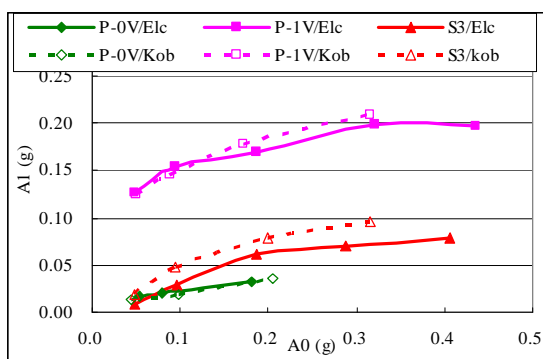
Test Name	Description
Elc	El Centro NS
Kobe	Kobe NS
TCU052	Chi-Chi – Station TCU052
TCU068	Chi-Chi – Station TCU068

Effectiveness of each control scheme can be determined from data collected during testing on the shake table. Data are presented in the following discussion first according to maximum response and, second, using time-history response. As numerous sensors are used, tabulation of performance indices facilitates comparison of the control schemes. To this end, a set of indices is used to define maximum values of the following quantities: (1) stroke of the MR damper ( $D_{mr}$ ), (2) relative displacement at the bottom of the isolated structure ( $D_1$ ), (3) relative displacement of the top of the isolated structure ( $D_2$ ), (4) input acceleration ( $A_0$ ), (5) absolute acceleration of the base of the isolated structure ( $A_1$ ), (6) absolute acceleration of the top of the isolated structure ( $A_2$ ) and (7) control force of the MR damper ( $L_{mr}$ ). Indices 1-3 are used to compare the control effect of maximum relative displacement. Relative displacements of the base and top of the isolated structure ( $D_1$  and  $D_2$ ) are the mean values of the measured responses from two LVDTs at each of the two levels. Indices 4-6 compare the degree of control of the maximum absolute acceleration. Absolute acceleration at the base and top of the isolated structure is also taken to be the mean value of the measured responses from two accelerometers at each level. Index 7 compares maximum force supplied by the MR damper.

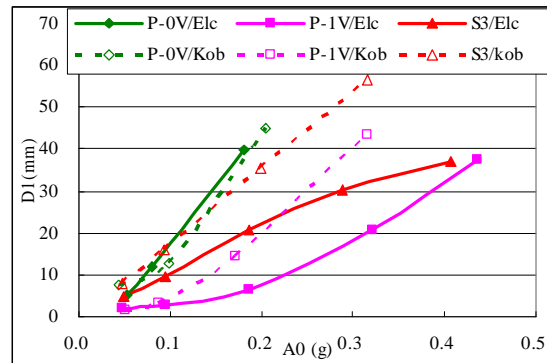
In order to facilitate comparison of results from a large number of experimental cases, Figures 5(a) and 6(a) show the relationships of maximum absolute acceleration ( $A_1$ ) of the isolated structure and maximum input ground acceleration ( $PGA/A_0$ ) for each excitation. Figure 5(b) and 6(b) show the relationships of maximum relative displacement ( $D_1/D_{mr}$ ) of the isolated structure and maximum input ground acceleration ( $PGA/A_0$ ) for each excitation. Plots in these figures for passive operation of the MR damper indicate only the two extremes of the voltage command levels, “P-off” and “P-on”, which represent the “lose power” and “maximum power” condition respectively. First, it is apparent from these figures that the greater the constant command voltage that is sent to the MR damper in a passive mode, the larger the reduction in relative displacement. Secondly, although the relative displacement is well controlled in the maximum command voltage case “P-on”, the control effect of

the absolute acceleration is poor. In short word, lower command voltage (such as case “P-off”) to the MR damper will lead better absolute acceleration reduction. But the stroke will exceed the capacity of the MR damper when the input ground acceleration exceeds 200 gal. Higher command voltage (such as case “P-on”) to the MR damper will lead better displacement reduction. But the absolute acceleration is always poor in every PGA level.

For semi-active control cases “S3”, reductions in the maximum relative displacement are similar in magnitude to the “P-on” case that uses the maximum command voltage, and the absolute acceleration of the isolated structure (A1) is almost as small as the case “P-off”. Moreover, since energy supplied to the MR damper can be reduced through use of modulated current, the semi-active control system provides a more efficient means of control than “P-on” and also reduces the temperature of the MR fluid. In conclusion, the semi-active controlled base-isolation system which uses the fuzzy logical control algorithm can control both the relative displacement and absolute acceleration. It is the most adaptable control system to control the base-isolation system subject to different PGA levels of excitations. It can adjust the command voltage to the MR damper to reduce the absolute acceleration in different PGA levels of excitations without exceeding the stroke capacity of the base-isolation system. In the other hand, the passive control cases can only control the relative displacement or the absolute acceleration. They are not adaptable to against different kinds of excitations

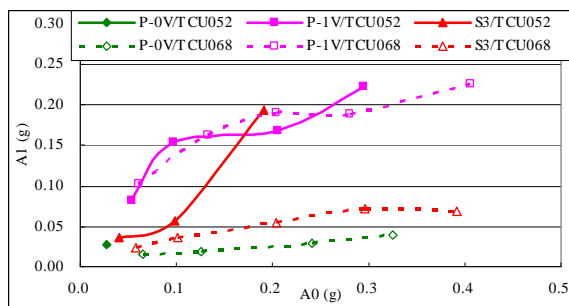


(a) Maximum acceleration of the isolated structure (A1)

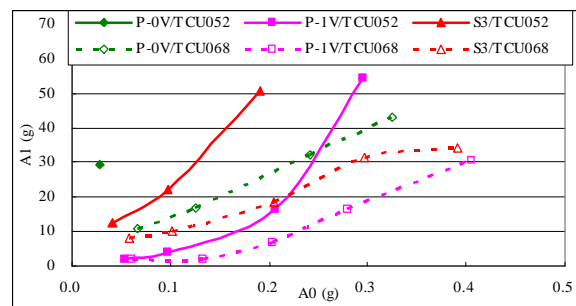


(b) Maximum relative displacement of the base-isolation system (D1)

Figure 5: Comparison of the maximum absolute acceleration (A1) and relative displacement (D1) of the hybrid controlled base-isolation system with different control cases (EQ cases: El Centro NS and Kobe NS).



(a) Maximum acceleration of the isolated structure (A1)



(b) Maximum relative displacement of the base-isolation system (D1)

Figure 6: Comparison of the maximum absolute acceleration (A1) and relative displacement (D1) of

the hybrid controlled base-isolation system with different control cases (EQ cases: Chi-Chi/Station: TCU052 and TCU068).

Time history of response from each transducer on the experimental structure provides additional data for interpretation of important phenomena. The discussion that follows first presents results from passive control and then those from semi-active control. The upper plot in Figure 7 shows the time history responses of the relative displacement of the passive-controlled (“P-1V”) base-isolation system under El Centro earthquake excitation (PGA=0.4g). While the lower plot shows the comparison of the input ground acceleration (red line) and the absolute acceleration of the base-isolated structure (green line). According to this figure, the passive controlled base-isolation system can subject to 400 gal El Centro earthquake excitation without exceeding the stroke capacity of the base-isolation system. The relative displacement control effect is good, and the absolute acceleration reduction is reduced from 400gals to 200 gals.

Figure 8 shows the same comparison in the semi-active controlled base-isolation system (“S3”). The time history response of the relative displacement is similar to the passive case “P-on” (See Figure 7). But, comparing the time history responses of the absolute accelerations, the maximum absolute acceleration response of the semi-active controlled base-isolated structure is greatly reduced from 400 gals to 80gals. It shows that the semi-active control system which uses the fuzzy logic control algorithm can reduce the relative displacement responses under strong earthquake excitation. In the same time, the acceleration reduction is not sacrificed. Figure 9 and 10 show the time history responses of the MR damper force (upper plot), command voltage (middle plot) and the hysteresis loops (lower left plot), force/velocity relationship of the MR damper in the passive (“P-1V”) and semi-active (“S3”) controlled base-isolation system under El Centro earthquake excitation. Comparing the time history responses of the MR damper forces in passive and semi-active control cases (see the upper plot in Figure 9 and 10), the damper force in passive mode is always huge, while the damper force in semi-active mode is altered according to the excitation. Comparing the command voltage to the MR damper (the middle plots in Figure 9 and 10). Passive case “P-on” always uses the great command level (1 Volt) as input, as result, the damper force is always huge. The command voltage of in the semi-active control case “S3” is altered according to the feedbacks from the responses of the base-isolation system and the fuzzy logical control gain (or, control surface). It make the MR damper can do the optimal adjustment in each time step, consequently, the semi-active control system will has the best control efficiency. The lower plot in figure 9 and 10 show the hysteresis loops and force/velocity relationships of the passive and semi-active control system. In figure 9, the MR damper is work in passive mode, as results, the hysteresis loop is unique just like a passive damper. In figure 10, the hysteresis loop is changing all the time. The shape of hysteresis loop is not only decided by the characteristic of the MR damper but also the fuzzy logic control gain. In this study, the hysteresis loop of the semi-active controlled MR damper has a bone shape. Which means, when the relative displacement is small the resistance of the MR damper is small to gain the better acceleration reduction. When the relative displacement is big, the resistance of the MR damper is big to mitigate the exceed displacement response.

## CONCLUSIONS

This experimental study investigates performance of a 12-ton mass supported by a hybrid base-isolation system that includes rolling pendulum system and a 20 kN MR damper. The system is tested on a large shake table and numerous transducers monitor motion and feedback data to a controller. Fuzzy logic control is used to design the semi-active controller that modulate voltage to

the MR damper. The goal is to mitigate response of the mass with the aid of the nonlinear base-isolation system. Different passive and semi-active control cases are used to test the effectiveness of each strategy.

Conclusions from this study are summarized as follows:

1. The rolling pendulum system is in place of the HDRB as the isolator in this study. It can provide a suitable restoring force with minimum friction force (or damping force). The damping force is only provided by the adjustable MR damper, and it can increase the controllable range of the semi-active control system
2. The benefit of a semi-active controllable damper in a base-isolation system is evident, especially for protection against different kinds of levels of earthquakes.
3. Semi-active controller S3, which considers both relative displacement and absolute acceleration, is the most effective controller used in this study. Not only can it control absolute acceleration for moderate levels of excitation, but it also mitigates relative displacement responses for large excitations and near-fault earthquakes.
4. Fuzzy logic control can be effective when used with a hybrid isolation system. Moreover, a semi-active controller can be custom-designed according to the desired performance criteria. For example, a controller can be designed to minimize both relative displacement and absolute acceleration similar to controller S3 or unequal weight can be assigned to different inputs.

This study provides evidence of full-scale, real-time control and highlights several advantages of augmenting a common base-isolation system with a semi-active MR damper that is modulated with a fuzzy controller.

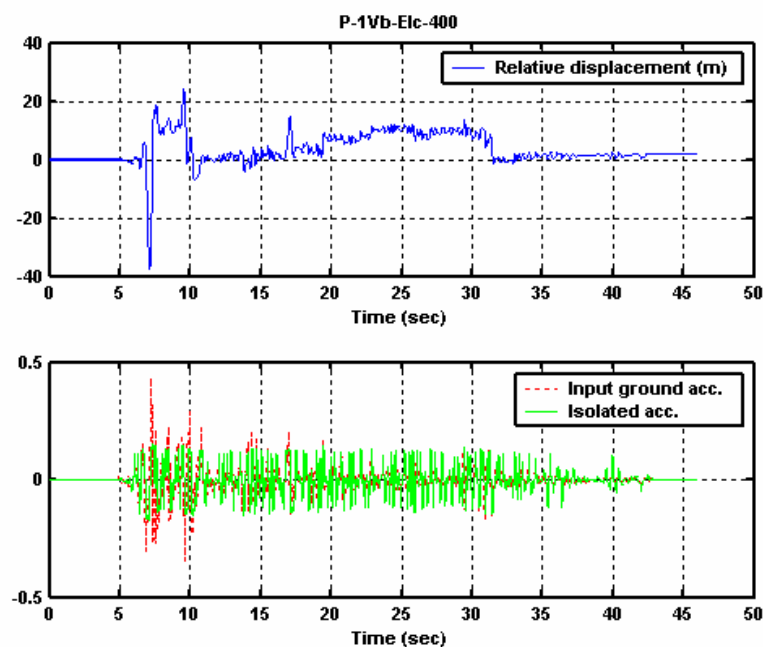


Figure 7: Time history responses of the relative displacement (upper plot), input ground acceleration and isolated acceleration (lower plot) of the passive-controlled (“P-1V”) base-isolation system under El Centro earthquake excitation (PGA=0.4g).

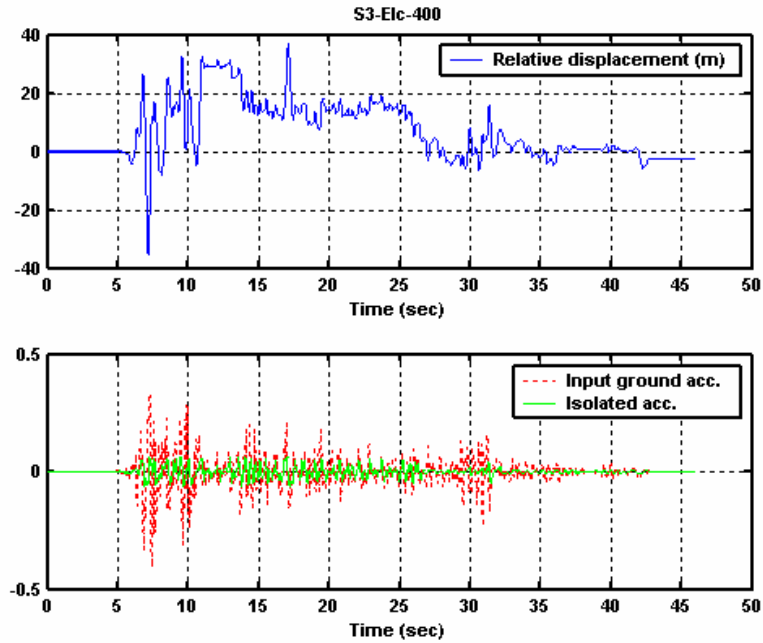


Figure 8: Time history responses of the relative displacement (upper plot), input ground acceleration and isolated acceleration (lower plot) of the semi-active controlled (“S3”) base-isolation system under El Centro earthquake excitation (PGA=0.4g).

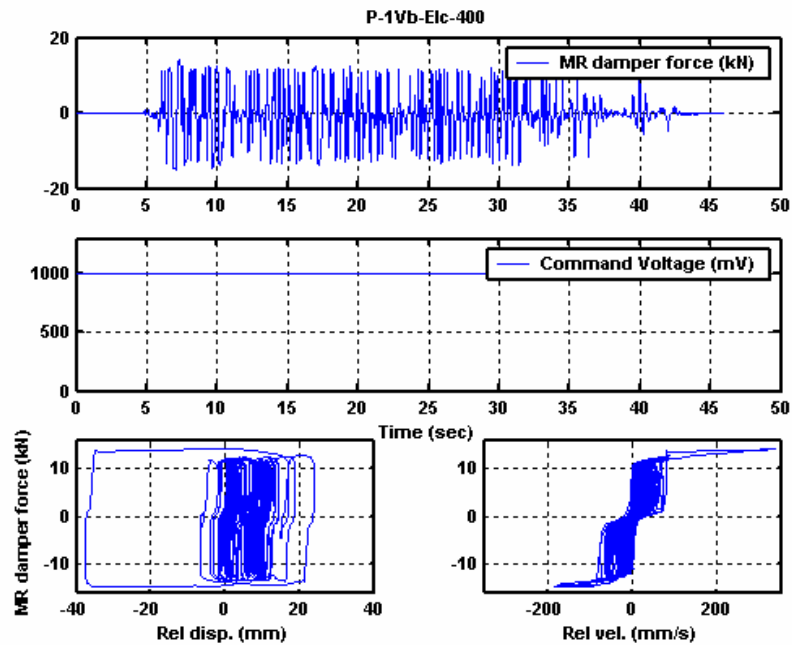


Figure 9: Time history responses of the MR damper force (upper plot), command voltage (middle plot) and the hysteresis loops (lower left plot), force/velocity relationship of the MR damper in the passive controlled (“P-1V”) base-isolation system under El Centro earthquake excitation (PGA=0.4g).

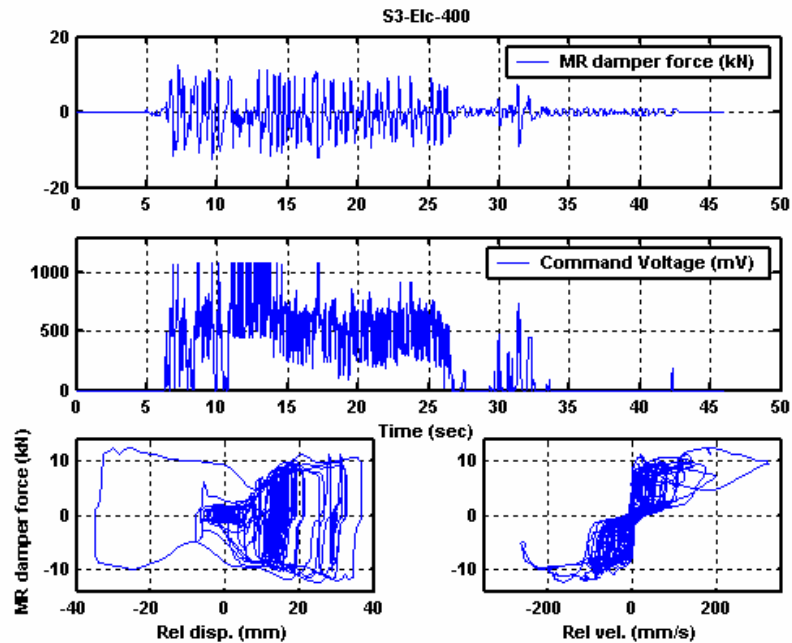


Figure 10: Time history responses of the MR damper force (upper plot), command voltage (middle plot) and the hysteresis loops (lower left plot), force/velocity relationship of the MR damper in the semi-active controlled (“S3”) base-isolation system under El Centro earthquake excitation (PGA=0.4g).

## ACKNOWLEDGEMENTS

The authors wish to express their thanks to the support by National Science Council, Taiwan, under NO.NSC 92A-0600000-26.

## REFERENCES

- Naeim F, Kelly JM. Design of Seismic Isolated Structures: from Theory to Practice. Wiley: New York, 1999.
- Chang SP, Makris N, Whittaker AS, and Thompson ACT, Experimental and analytical studies on the performance of hybrid isolation systems, *Earthquake Engineering and Structural Dynamics*, 2002, 31:421-443.
- Sadek, F, and Mohraz B, Semiactive control algorithm for structures with variable dampers, *Journal of Engineering Mechanics*, Sep., 1998, pp. 981-990.
- Symans MD, Constantinou MC, Seismic testing of a building structure with a semi-active fluid damper control system, *Earthquake Engineering and Structural Dynamics*, 1997, 26:759-777.
- Kurata N, Kobori T, Takahashi M, Niwa N, and Midorikawa H., Actual seismic response of controlled building with semi-active damper system, *Earthquake Engineering and Structural Dynamics*, 1999, 28:1427-1447.
- Niwa N, Kobori T, Takahashi M, Midorikawa H, Kurata N, and Mizuno T, Dynamic loading test and simulation analysis of full-scale semi-active hydraulic damper for structural control, *Earthquake Engineering and Structural Dynamics*, 2000, 29:789-812.

Kobori T, Takahashi M, Nasu T, and Niwa N, Seismic response controlled structure with active variable stiffness system, *Earthquake Engineering and Structural Dynamics*, 1993, 22:925-941.

Burton SA, Makris N, Konstantopoulos I, and Antsaklis PJ, Modeling the response of ER damper: phenomenology and emulation, *Journal of Engineering Mechanics*, Sep. 1996, pp. 897-906.

Spencer, Jr BF, Dyke SJ, Sain MK, and Carlson JD, Phenomenological model of magnetorheological dampers, *Journal of Engineering Mechanics*, ASCE, 1997, 123(3):230-238.

Chang CC, Roschke PN, Neural network modeling of a magnetorheological damper, *Journal of Intelligent Material Systems and Structures*, 1998, 9:755-764.

Wang, Y. P., Chung, L. L. and Liao, W. H., "Seismic response analysis of bridges isolated with friction pendulum bearings," *Earthquake Engineering and Structural Dynamics*, Oct., 1998, 27(10), pp. 1069-1093.

Lin PY, Loh CH, Chung LL, Chang CP, and Roschke PN, Semi-active controlled base-isolation system with magnetorheological damper, Report Number NCREE-03-015, National Center for Research on Earthquake Engineering, Taipei, Taiwan, 2003.

Fuzzy Logic Toolbox Users Guide, The MathWorks, Inc.